

Influence of statistical fluctuation on reproducibility and accuracy of SUV_{max} and SUV_{peak} : a phantom study

Go Akamatsu^{1,2}, Yasuhiko Ikari¹, Hiroyuki Nishida¹, Tomoyuki Nishio¹, Akihito Ohnishi¹, Akira Maebatake², Masayuki Sasaki², Michio Senda¹

1. Division of Molecular Imaging, Institute of Biomedical Research and Innovation
2. Department of Health Sciences, Graduate School of Medical Sciences, Kyushu University

Corresponding author:

Michio Senda, MD, PhD

Division of Molecular Imaging, Institute of Biomedical Research and Innovation

2-2, Minatojima-Minamimachi, Chuo-ku, 650-0047, Kobe, Japan

TEL: +81-78-304-5212, FAX: +81-78-304-5201

E-mail: senda@fbri.org

First author:

Go Akamatsu, MS

Division of Molecular Imaging, Institute of Biomedical Research and Innovation

2-2, Minatojima-Minamimachi, Chuo-ku, 650-0047, Kobe, Japan

TEL: +81-78-304-5212, FAX: +81-78-304-5201

E-mail: akamatsu@fbri.org, golilin5@gmail.com

Department of Health Sciences, Graduate School of Medical Sciences, Kyushu University

3-1-1, Maidashi, Higashi-ku, 812-8582, Fukuoka, Japan

Ph.D. Student

The word count of the manuscript: 3345 words

RUNNING FOOT LINE: Effect of Statistical Noise on SUV

This study was supported in part by “Fukuoka Foundation for Sound Health” cancer research fund.

ABSTRACT

Standardized uptake values (SUV) have been widely used in diagnosis of malignant tumors and in clinical trials of tumor therapies as a semi-quantitative metrics of tumor FDG uptake. However, SUV for small lesions is liable to errors due to partial volume effect and statistical noise. The purpose of this study was to evaluate the reproducibility and accuracy of SUV_{max} and SUV_{peak} of small lesions in phantom experiments. **Methods:** We used a NEMA IEC body phantom with 6 spheres in 1/4 warm background. The PET data were acquired for 1,800 seconds in a list-mode, from which data were extracted to generate a total of 15 PET images for each of 60, 90, 120, 150, and 180 second scanning time. The SUV_{max} and SUV_{peak} of the hot spheres in the 1,800 second scan were used as a reference ($SUV_{ref, max}$ and $SUV_{ref, peak}$). Coefficients of variation for both SUV_{max} and SUV_{peak} in hot spheres (CV_{max} and CV_{peak}) were calculated to evaluate the variability of the SUVs. On the other hand, percent differences between SUV_{max} and $SUV_{ref, max}$ and between SUV_{peak} and $SUV_{ref, peak}$ were calculated for evaluation of the accuracy of SUV ($\%Diff_{max}$ and $\%Diff_{peak}$). We additionally examined the coefficients of variation of background activity ($CV_{background}$) and the percent background variability (N_{10mm}) as parameters for the physical assessment of image quality. **Results:** Visibility of a 10-mm-diameter hot sphere was considerably

different among scan frames. The CV_{\max} and CV_{peak} increased as the sphere size became smaller and as the acquisition time became shorter. SUV_{\max} were generally overestimated as the scan time shortened and the sphere size increased. The SUV_{\max} and SUV_{peak} of 37-mm-diameter sphere for 60-second scans had average positive biases of 28.3% and 4.4% compared with the reference. **Conclusion:** SUV_{\max} was variable and overestimated as the scan time decreased and the sphere size increased. In contrast, SUV_{peak} was a more robust and accurate metric than SUV_{\max} . The measurements of SUV_{peak} (or SUL_{peak}) in addition to SUV_{\max} are desirable for reproducible and accurate quantification in clinical situations.

Key Words: SUV_{\max} ; SUV_{peak} ; FDG-PET; statistical fluctuation; reproducibility

Whole-body oncologic ^{18}F -FDG-PET is useful for detection and staging of various malignant tumors, monitoring of responses to therapy and prognostic stratification (1–4). Standardized uptake values (SUV) have been widely used for diagnosing malignant tumors and for clinical trials of tumor therapies as a semi-quantitative metrics of tumor ^{18}F -FDG uptake (1,5,6). Recently, SUV has been used to monitor metabolic response to therapy (1,6). Although SUV is easy to derive tumor metabolic changes (5), accurate and reproducible quantification is crucial to the clinical evaluation of sequential PET/CT imaging.

Positron emission itself is characterized statistically by a Poisson distribution (7). Even if the same object is scanned, the same image cannot be obtained due to the statistical fluctuation (8). It is important to reduce the variability and to improve the accuracy of SUV by sufficient scan duration (8). Under the current guideline (9,10) on phantom experiment, the PET image quality is generally evaluated by the percent contrast ($Q_{\text{H}, 10\text{mm}}$) and the percent background variability ($N_{10\text{mm}}$). Various organizations including Society of Nuclear Medicine and Molecular Imaging/Clinical Trial Network (11), the European Association of Nuclear Medicine/EANM Research Ltd (12) and the American College of Radiology/ACR Imaging Network (13) evaluated the accuracy of SUV with the aim of the harmonization of quantitative values (14). Although the $Q_{\text{H}, 10\text{mm}}$, $N_{10\text{mm}}$ and the accuracy of SUV are

important metrics of good image quality, the reproducibility of small lesion uptake is also essential. In general, SUV_{max} is considered to be overestimated in low count statistics images because the highest pixel value tends to present high values due to noise (15). A previous clinical study by Lodge et al. (16) indicated that maximum SUV (SUV_{max}) was overestimated in low count statistics images. Boellaard et al. (15) also reported that SUV_{max} showed positive bias for images with higher noise. However, relationship among scan time, image noise, lesion size and variability of SUV_{max} and peak SUV (SUV_{peak}) has not been investigated yet. The purpose of this study was to evaluate the reproducibility and accuracy of SUV_{max} and SUV_{peak} of small lesions using a phantom.

MATERIALS AND METHODS

Imaging Protocols

In this study, we used a Discovery-690 PET/CT scanner (GE Healthcare, Milwaukee, WI) and National Electrical Manufacturers Association/International Electrotechnical Commission body phantom (Data Spectrum Corp.). The PET scanner comprises a total of 13,824 LYSO crystals with dimensions of $4.2 \times 6.3 \times 25$ mm³, covering an axial field-of-view (FOV) of 15.7 cm and a transaxial FOV of 70 cm in diameter. The

coincidence time window was 4.9 ns. The TOF time resolution was 544.3 ps. The NEMA body phantom with a lung insert and 6 spheres of 37, 28, 22, 17, 13, and 10 mm inner diameter had a background activity of 2.65 kBq/mL at 15 min from scan start time. The activity level simulated injection dose of 3.7 MBq/kg (9,10). The sphere-to-background ratio was 4:1. The whole inner volume of the phantom was 9,780 mL. The PET data were acquired for 30 min in list-mode, and reconstructed by using the ordered subsets expectation maximization (OSEM) plus time-of-flight (TOF) algorithm with 3 iterations and 8 subsets. A total of 15 PET images were reconstructed for each scan time of 60, 90, 120, 150, and 180 sec from the 30 min list-mode data, respectively (Fig. 1). The image matrix was 192×192 with a 3.12 mm pixel size. The display FOV (DFOV) was 60.0 cm. The PET image slice thickness was 3.27 mm. A Gaussian filter of 4 mm FWHM was used as a post-smoothing filter. CT scan was performed using the following parameters: 120 kV, 40 mA, 0.5-s tube rotation, and 5-mm slice collimation. The CT data were used for the attenuation correction.

Image Analysis

We analyzed the SUV_{max} and SUV_{peak} of all spheres using the PET Volume

Computer Assisted Reading software (GE Healthcare). The SUV_{peak} was calculated with the mean value of 12-mm-diameter sphere volume of interest (VOI) positioned so as to maximize the enclosed average activity. The SUV_{peak} of 10-mm-diameter sphere ($SUV_{\text{peak},10}$) was not evaluated because the predetermined VOI with 12-mm-diameter was larger than the 10-mm-diameter sphere. Coefficients of variation (CV) of the SUV of each sphere were calculated for evaluation of variability of the SUV as follows:

$$CV_{\text{max},j} = [(\text{SD of } SUV_{\text{max},j}) / (\text{Mean of } SUV_{\text{max},j})] \times 100 (\%)$$

$$CV_{\text{peak},j} = [(\text{SD of } SUV_{\text{peak},j}) / (\text{Mean of } SUV_{\text{peak},j})] \times 100 (\%)$$

where j is a diameter of the sphere and SD is the standard deviation.

The maximum and peak SUV of j -mm-diameter in 1,800 sec scan data were defined as the reference maximum and peak SUV ($SUV_{\text{ref, max}, j}$ and $SUV_{\text{ref, peak}, j}$, respectively). Then, differences between the $SUV_{\text{max}, j}$ and $SUV_{\text{ref, max}, j}$ and between $SUV_{\text{peak}, j}$ and $SUV_{\text{ref, peak}, j}$ were calculated for evaluation of accuracy of the SUV as follows:

$$\%Diff_{\text{max},j} = \text{mean of } [| SUV_{\text{max},j} - SUV_{\text{ref, max},j} | / SUV_{\text{ref, max},j}] (\%)$$

$$\%Diff_{\text{peak},j} = \text{mean of } [| SUV_{\text{peak},j} - SUV_{\text{ref, peak},j} | / SUV_{\text{ref, peak},j}] (\%)$$

The physical assessment of the PET image quality was additionally performed

with the coefficient of variation of background activity ($CV_{\text{background}}$) and the percent background variability ($N_{10\text{mm}}$) (9,10). We placed 12 circular regions of interest (ROIs) of 30 mm and 10 mm in diameter on the central slice and on ± 1 cm and ± 2 cm away from the central one (total of 120 ROIs) in each PET image. The $CV_{\text{background}}$ was calculated using the data of 30-mm ROIs as follows:

$$CV_{\text{background}} = \text{mean of } [(SD / \text{mean}) \times 100] (\%)$$

The $N_{10\text{mm}}$ was calculated using the data of 10-mm ROIs as follows:

$$N_{10\text{mm}} = SD_{10\text{mm}} / C_{B,10\text{mm}} \times 100 (\%)$$

where $C_{B,10\text{mm}}$ is the mean measured activity in the ROI for the 10-mm-diameter sphere in background 12 ROIs on the central slice. $SD_{10\text{mm}}$ is the SD of the background ROI values for 10-mm-diameter sphere.

RESULTS

Figure 2 illustrates all the PET images for various scanning durations. The PET image quality was improved as the scanning time increased. Visibility of the 10-mm-diameter hot sphere was considerably different among the frames of the same scanning time. Figure 3A showed representative images with different $SUV_{\text{max},10}$. Although

both images were acquired for 60 seconds, $SUV_{max, 10}$ varied from 1.92 to 2.85. Figure 3B illustrated 3-dimensional (3D) graph of the activity of the 37-mm-diameter sphere in the 1,800 sec scan image and in the 60 sec scan image. A maximum value of a hot sphere in the low count statistics image was often higher than that in the high count statistics image (Fig. 3B).

The variability of SUV_{max} and SUV_{peak} of the hot spheres and that of mean SUV of the background in relation to the scanning time were shown in Table 1. The variability of both SUV_{max} and SUV_{peak} increased as the sphere size became smaller and as the scanning time became shorter. When the $CV_{background}$ was 10% or lower, all of the CV_{max} and CV_{peak} were lower than 10%. It took 150 seconds or longer scanning time for small spheres to have the CV_{max} of 10% or lower. On the other hand, all of the CV_{peak} was lower than 5% regardless of the scanning time and sphere size.

Table 2 and Figure 4 show the accuracy of both SUV_{max} and SUV_{peak} in relation to the scanning time and the sphere size. The $\%Diff_{max}$ showed that the SUV_{max} were generally overestimated as the scanning time shortened and the sphere size became larger. In particular, the $SUV_{max, 37}$ by 60 sec scan showed 28.3% overestimation compared with the $SUV_{ref, max, 37}$. In contrast, the $\%Diff_{peak}$ showed minimal overestimation. The $SUV_{peak, 37}$

was overestimated by 4.4%. A 180-second or longer scan time was required to achieve the recommended $N_{10\text{mm}}$ of 6.3% for 2.65 kBq/mL background concentration in the guideline (Table 1). Although the $N_{10\text{mm}}$ achieved the recommended value, the CV_{max} and $\%Diff_{\text{max}, 37}$ were 8.5% and 12.3%, respectively.

DISCUSSION

Our phantom study evaluated the reproducibility and accuracy of SUV_{max} and SUV_{peak} in hot spheres simulating ^{18}F -FDG avid tumors. To achieve the CV of 10% or lower, the required scanning time was 150 sec or longer for SUV_{max} and 60 sec or longer for SUV_{peak} . We found that SUV_{max} was variable and overestimated even in the images which satisfied the guideline-recommended image quality. Although many studies attempted to minimize technical factors affecting accuracy of SUV for the purpose of harmonization of quantitative values (5,12–14,17), minimizing the variability of SUVs are also important for multicenter PET studies such as clinical evaluation of new PET tracers and new applications of the PET technique (18). On the other hand, SUV_{peak} was more robust for statistical fluctuation than SUV_{max} .

The variability of SUV_{max} in hot spheres was higher as the scanning time shortened in this study. On images with high background variability, SUV_{max} in hot spheres showed high variability. Furthermore, the SUV_{max} resulted in large overestimations as the image noise increased. The SUV_{max} of the 37-mm-diameter sphere with 60 sec scan showed 28.3% overestimation compared with that with 1,800 sec scan. These results were consistent with a previous simulation study reported by Boellaard, et al. (15). Many studies

have also reported that SUV_{max} in small lesions strongly depended on image noise (15,16,19–21). In this study, the variability of the SUV_{max} in hot spheres was higher as the hot sphere became smaller. The SUV_{max} in small lesions were underestimated due to partial volume effect (21,22). The higher variability of SUV_{max} in small spheres must be due to the fluctuation in low count statistics in comparison with the large spheres. Many PET examinations have been performed to detect small lesions and to evaluate responses to therapy for small lesions in both clinical trials and clinical practice (23). It is important to obtain sufficient reproducibility of SUV_{max} in small lesions. The image noise levels depended on the scanning time. Based on these results, determination of the appropriate scan time is important for assuring reproducibility and accuracy of SUV_{max} .

The variability in the background area was evaluated using the CV and N_{10mm} in this study. Quantitative Imaging Biomarkers Alliance/Uniform Protocol in Clinical Trial (QIBA/UPICT) recommends that the CV in the uniform area should ideally yield below 10% (24). When the $CV_{background}$ was smaller than 10%, the CV of SUV_{max} in hot spheres also resulted in below 10% in this study. On the other hand, the Japanese guideline (10) recommends that the N_{10mm} should achieve 6.3% or lower for NEMA body phantom with 2.65 kBq/mL background activity. When the N_{10mm} satisfied the criterion, the CV of

SUV_{max} was also below 10% in this study. A scanning time of 180 sec or longer was required to satisfy the criteria of $CV_{background}$ or N_{10mm} in this study. Although the $CV_{background}$ or N_{10mm} achieved the recommendation, the $CV_{max, 10}$ and $\%Diff_{max, 37}$ were 8.5% and 12.3%, respectively. These uncertainties have a potential influence on the assessment of metabolic response based on the relative change in SUV_{max} .

Many studies for response assessment in clinical trials adopted SUV_{max} for quantification due to many advantages of SUV_{max} (16,21,25,26). In this study, the variability of SUV_{peak} was smaller than that of SUV_{max} although the SUV_{peak} showed close correlation with the SUV_{max} . Several studies have also reported that SUV_{peak} was more robust to the statistical fluctuation than SUV_{max} (16,27). In contrast to the SUV_{max} , the SUV_{peak} showed less than 5% overestimation on all scanning time and sphere size. Based on these results, SUV_{peak} were considered to be more reproducible and accurate metric than SUV_{max} . Several studies have also reported that SUV_{peak} was a more robust alternative (16) because it has been expected to reduce uncertainties in the quantification of responses to therapy (16,19,25,27). Vanderhoek, et al. (27) emphasized that the most robust and predictive method of SUV measurement should be selected for quantification of responses to therapy in clinical trials. Furthermore, the ^{18}F -FDG PET/CT UPICT protocol (24)

recommends that SUV_{peak} for 3D volume should be obtained in addition to SUV_{max} in clinical trials. The use of SUV_{peak} is suitable especially for the purpose of harmonizing the quantitative performance of various PET scanners. In PERCIST, the measurement of SUV_{peak} normalized to lean body mass (SUL_{peak}) are recommended to assess response to therapy (28). Although there were limitations in applicability to small lesions (below 12-mm-diameter) and requirement for the dedicated image analysis software, we recommend that the measurements of SUV_{peak} (or SUL_{peak}) in addition to SUV_{max} are desirable for reproducible and accurate quantification in clinical situations. It would improve diagnostic accuracy if both SUV_{max} and SUV_{peak} were evaluated (27).

In this study, we adopted the 1-cm³-volume VOI in order to compare with previous studies. However, several studies used various VOI sizes to calculate SUV_{peak} (15,19,27). A further study to determine the ideal VOI size for the SUV_{peak} is necessary for standardization of quantitative performance.

This study did not take the subject size into consideration. However, the PET image quality of overweight subjects (body mass index ≥ 25) is degraded due to an increase in statistical noise (29–31). In order to obtain sufficient image quality, adjusting the injection activity and/or scanning time in each patient based on their body weight or body

mass index (29,32,33) might be required for overweight subjects (34,35). SUV was increased as a function of patient weight based on a simulation study reported by Boellaard et al. (15). A further clinical study is required to examine the reproducibility and accuracy of the SUV.

CONCLUSION

SUV_{max} is variable and overestimated as the scanning time decreases and the lesion size enlarges. While the standardization and harmonization of quantitative oncology ^{18}F -FDG-PET imaging protocols are on the focus, sufficient scanning time is required to obtain enough reproducibility and accuracy of SUVs of small lesions. We suggest that CV in the uniform area of the appropriate phantom should be below 10% to minimize the effect of statistical fluctuation for the SUV_{max} . On the other hand, SUV_{peak} is a more robust and accurate metric than SUV_{max} . Measurement of SUV_{peak} (or SUL_{peak}) in addition to SUV_{max} is desirable for reproducible and accurate quantification in clinical trials.

DISCLOSURE

This study was supported in part by “Fukuoka Foundation for Sound Health” cancer research fund. No other potential conflict of interest relevant to this article reported.

REFERENCES

1. Hicks RJ. Role of 18F-FDG PET in assessment of response in non-small cell lung cancer. *J Nucl Med*. 2009;50 Suppl 1:31S–42S.
2. Rohren EM, Turkington TG, Coleman RE. Clinical applications of PET in Oncology. *Radiology*. 2004;231:305–332.
3. Fischer B, Lassen U, Mortensen J, et al. Preoperative staging of lung cancer with combined PET-CT. *N Engl J Med*. 2009;361:32–39.
4. Kitajima K, Kita M, Suzuki K, Senda M, Nakamoto Y, Sugimura K. Prognostic significance of SUVmax (maximum standardized uptake value) measured by [¹⁸F]FDG PET/CT in endometrial cancer. *Eur J Nucl Med Mol Imaging*. 2012;39:840–845.
5. Lasnon C, Desmots C, Quak E, et al. Harmonizing SUVs in multicentre trials when using different generation PET systems : prospective validation in non-small cell lung cancer patients. *Eur J Nucl Med Mol Imaging*. 2013;40:985–996.
6. Weber WA, Petersen V, Schmidt B, et al. Positron emission tomography in non-small-cell lung cancer: prediction of response to chemotherapy by quantitative assessment of glucose use. *J Clin Oncol*. 2003;21:2651–2657.
7. Teymurazyan A, Riauka T, Jans HS, Robinson D. Properties of noise in positron emission tomography images reconstructed with filtered-backprojection and row-action maximum likelihood algorithm. *J Digit Imaging*. 2013;26:447–456.
8. Schwartz J, Humm JL, Gonen M, et al. Repeatability of SUV measurements in serial PET. *Med Phys*. 2011;38:2629–2638.
9. NEMA standards publication NU 2-2012: performance measurements of positron emission tomographs. Rosslyn, VA: National Electrical Manufacturers Association; 2012.

10. Fukukita H, Suzuki K, Matsumoto K, et al. Japanese guideline for the oncology FDG-PET/CT data acquisition protocol: synopsis of Version 2.0. *Ann Nucl Med*. 2014;28:693–705.
11. Graham MM. The Clinical Trials Network of the Society of Nuclear Medicine. *Semin Nucl Med*. 2010;40:327–331.
12. Boellaard R, O’Doherty MJ, Weber WA, et al. FDG PET and PET/CT: EANM procedure guidelines for tumour PET imaging: version 1.0. *Eur J Nucl Med Mol Imaging*. 2010;37:181–200.
13. Scheuermann JS, Saffer JR, Karp JS, Levering AM, Siegel BA. Qualification of PET scanners for use in multicenter cancer clinical trials: the American College of Radiology Imaging Network experience. *J Nucl Med*. 2009;50:1187–1193.
14. Makris NE, Huisman MC, Kinahan PE, Lammertsma AA, Boellaard R. Evaluation of strategies towards harmonization of FDG PET/CT studies in multicentre trials: comparison of scanner validation phantoms and data analysis procedures. *Eur J Nucl Med Mol Imaging*. 2013;40:1507–1515.
15. Boellaard R, Krak NC, Hoekstra OS, Lammertsma AA. Effects of noise, image resolution, and ROI definition on the accuracy of standard uptake values: a simulation study. *J Nucl Med*. 2004;45:1519–1527.
16. Lodge MA, Chaudhry MA, Wahl RL. Noise considerations for PET quantification using maximum and peak standardized uptake value. *J Nucl Med*. 2012;53:1041–1047.
17. Kelly MD, Declerck JM. SUVref: reducing reconstruction-dependent variation in PET SUV. *EJNMMI Res*. 2011;1:16.
18. Boellaard R. Standards for PET image acquisition and quantitative data analysis. *J Nucl Med*. 2009;50 Suppl 1:11S–20S.

19. Krak NC, Boellaard R, Hoekstra OS, Twisk JW, Hoekstra CJ, Lammertsma AA. Effects of ROI definition and reconstruction method on quantitative outcome and applicability in a response monitoring trial. *Eur J Nucl Med Mol Imaging*. 2005;32:294–301.
20. Adams MC, Turkington TG, Wilson JM, Wong TZ. A systematic review of the factors affecting accuracy of SUV measurements. *AJR Am J Roentgenol*. 2010;195:310–320.
21. Soret M, Bacharach SL, Buvat I. Partial-volume effect in PET tumor imaging. *J Nucl Med*. 2007;48:932–945.
22. Keyes JW Jr. SUV: standard uptake or silly useless value? *J Nucl Med*. 1995;36:1836–1839.
23. Weber WA. Positron emission tomography as an imaging biomarker. *J Clin Oncol*. 2006;24:3282–3292.
24. ¹⁸F-FDG PET/CT UPICT Protocol Writing Committee. UPICT Oncology FDG-PET CT Protocol.
http://qibawiki.rsna.org/images/d/de/UPICT_Oncologic_FDG-PETCTProtocol_6-07-13.pdf.
25. Nahmias C, Wahl LM. Reproducibility of standardized uptake value measurements determined by ¹⁸F-FDG PET in malignant tumors. *J Nucl Med*. 2008;49:1804–1808.
26. Safar V, Dupuis J, Itti E, et al. Interim [¹⁸F]fluorodeoxyglucose positron emission tomography scan in diffuse large B-cell lymphoma treated with anthracycline-based chemotherapy plus rituximab. *J Clin Oncol*. 2012;30:184–190.
27. Vanderhoek M, Perlman SB, Jeraj R. Impact of the definition of peak standardized uptake value on quantification of treatment response. *J Nucl Med*. 2012;53:4–11.

28. Wahl RL, Jacene H, Kasamon Y, Lodge MA. From RECIST to PERCIST: Evolving Considerations for PET response criteria in solid tumors. *J Nucl Med*. 2009;50 Suppl 1:122S–150S.
29. Halpern BS, Dahlbom M, Quon A, et al. Impact of patient weight and emission scan duration on PET/CT image quality and lesion detectability. *J Nucl Med*. 2004;45:797–801.
30. El Fakhri G, Santos PA, Badawi RD, Holdsworth CH, Van Den Abbeele AD, Kijewski MF. Impact of acquisition geometry, image processing, and patient size on lesion detection in whole-body 18F-FDG PET. *J Nucl Med*. 2007;48:1951–1960.
31. Taniguchi T, Akamatsu G, Kasahara Y, et al. Improvement in PET/CT image quality in overweight patients with PSF and TOF. *Ann Nucl Med*. 2015;29:71–77.
32. Halpern BS, Dahlbom M, Auerbach MA, et al. Optimizing imaging protocols for overweight and obese patients: a lutetium orthosilicate PET/CT study. *J Nucl Med*. 2005;46:603–607.
33. Tatsumi M, Clark PA, Nakamoto Y, Wahl RL. Impact of body habitus on quantitative and qualitative image quality in whole-body FDG-PET. *Eur J Nucl Med Mol Imaging*. 2003;30:40–45.
34. Masuda Y, Kondo C, Matsuo Y, Uetani M, Kusakabe K. Comparison of imaging protocols for 18F-FDG PET/CT in overweight patients: optimizing scan duration versus administered dose. *J Nucl Med*. 2009;50:844–848.
35. Nagaki A, Onoguchi M, Matsutomo N. Patient weight-based acquisition protocols to optimize (18)F-FDG PET/CT image quality. *J Nucl Med Technol*. 2011;39:72–76.

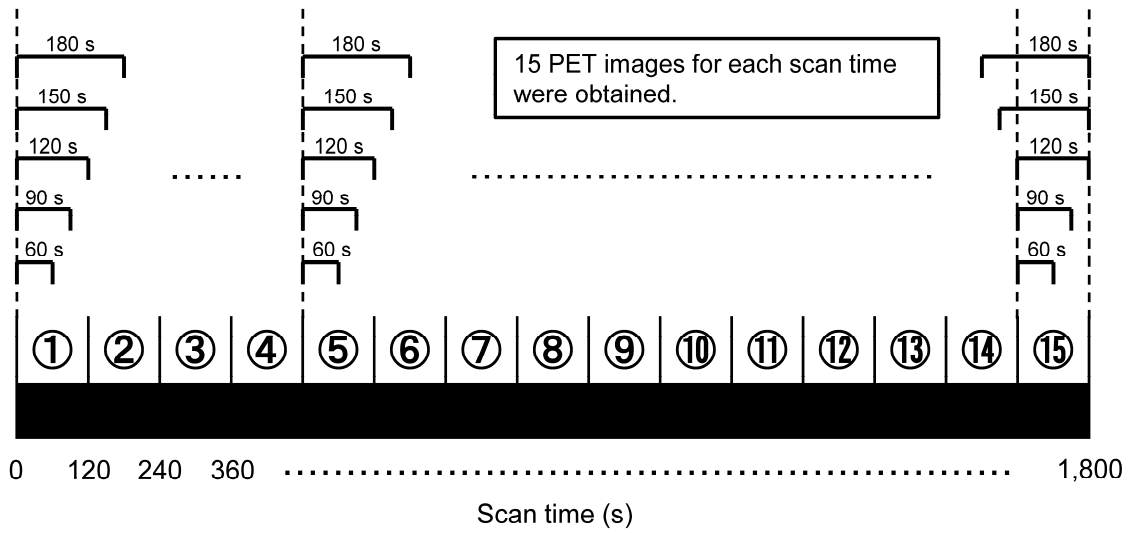


FIGURE 1. Method of extracting PET acquisition data of various scan time from a long list-mode data. Fifteen PET images for each scan time were generated, making a total of 76 PET images.

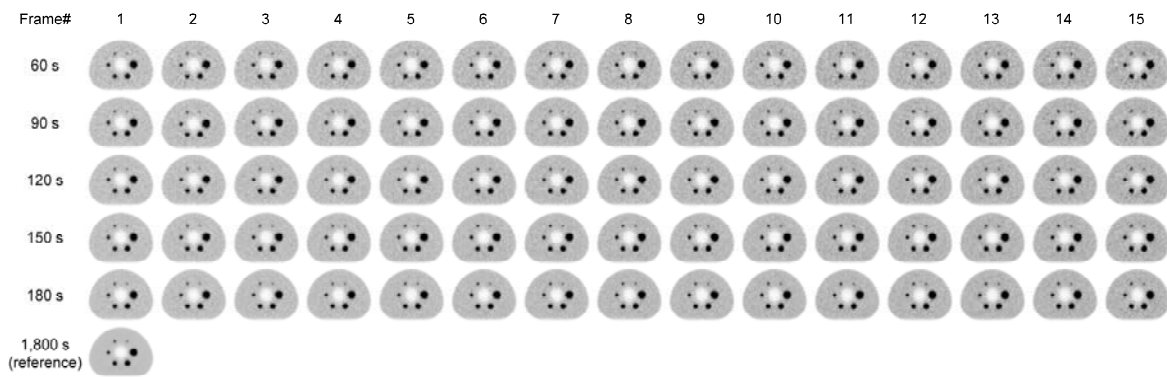


FIGURE 2. All PET images obtained in this study are shown. Images are not identification even with the same scanning time. Visualization of hot spheres depend on the scanning time.

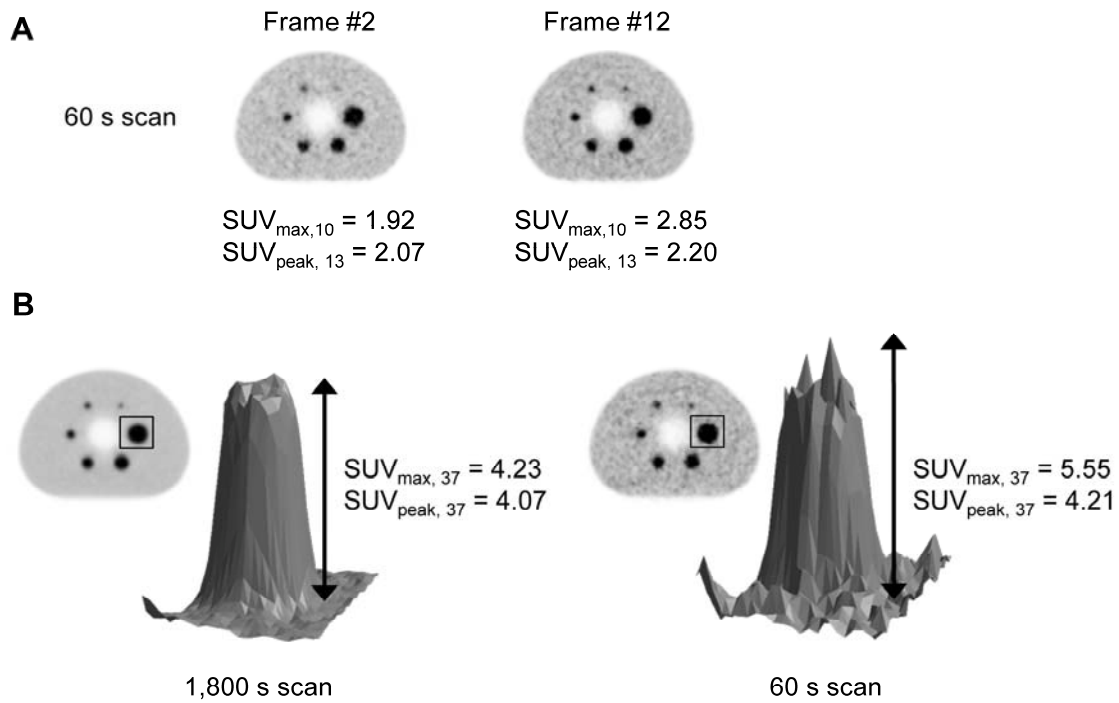


FIGURE 3. (A) PET images having highest (#12) and lowest (#2) $SUV_{max,10}$ value among the 15 frames of 60 sec scan. The $SUV_{max,10}$ fluctuate up and down considerably. (B) Three-dimensional graphics of the 37-mm-diameter hot sphere with 1,800 sec scan and 60 sec scan. The maximum pixel value of a small hot sphere in a low count statistics image was often higher than that in the high count statistics image.

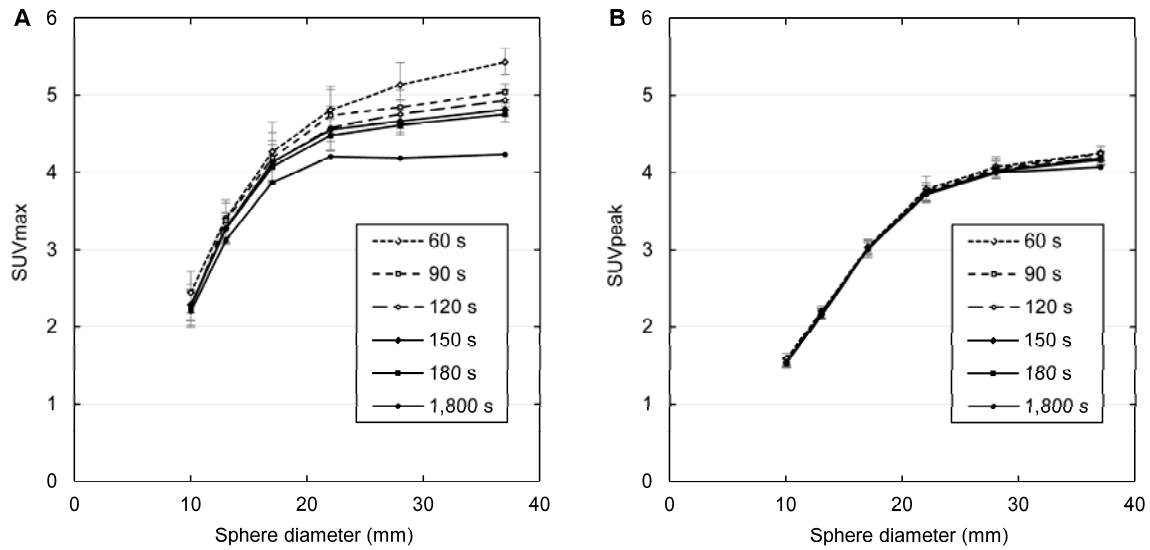


FIGURE 4. SUV_{max} and SUV_{peak} in relation to sphere sizes and scan times. The $SUV_{max, 37}$ for the 60 sec image had positive biases of 28.3% compared with the $SUV_{ref, max, 37}$. SUV_{max} were overestimated as the sphere size increased and the scanning time decreased. SUV_{peak} was almost constant irrespective of the scan time.

TABLE 1

Variability (Coefficient of variation) of SUV_{max} and SUV_{peak} of the hot spheres and background in relation to scanning time.

	Scan time (sec)				
	60	90	120	150	180
$CV_{max, 10}$	11.0	10.9	11.6	8.8	8.5
$CV_{max, 13}$	7.0	6.7	6.0	6.2	5.3
$CV_{max, 17}$	8.8	7.9	7.0	5.6	4.8
$CV_{max, 22}$	6.3	7.1	6.2	5.9	4.5
$CV_{max, 28}$	5.7	4.5	3.9	3.0	2.7
$CV_{max, 37}$	3.1	2.0	2.7	1.8	2.1
$CV_{peak, 13}$	3.5	3.6	3.5	3.4	2.7
$CV_{peak, 17}$	3.3	3.8	3.4	2.8	2.1
$CV_{peak, 22}$	4.6	3.0	2.7	2.7	2.9
$CV_{peak, 28}$	3.1	3.1	2.8	2.1	2.2
$CV_{peak, 37}$	2.3	2.4	2.1	2.2	1.5
$CV_{background}$	16.5	13.6	11.8	10.7	9.8
N_{10mm}	10.1	8.5	7.6	6.9	6.1

TABLE 2Accuracy of SUV_{max} and SUV_{peak} in relation to scanning time.

	Scan time (sec)				
	60	90	120	150	180
%Diff _{max, 10}	12.9	8.5	8.4	7.0	7.2
%Diff _{max, 13}	9.4	9.1	6.9	6.4	6.0
%Diff _{max, 17}	11.0	9.1	7.5	7.0	5.7
%Diff _{max, 22}	14.4	12.8	8.9	8.4	6.6
%Diff _{max, 28}	22.7	15.9	13.7	11.4	10.2
%Diff _{max, 37}	28.3	19.1	16.6	13.7	12.3
%Diff _{peak, 13}	3.7	3.5	3.1	2.8	2.3
%Diff _{peak, 17}	2.8	2.7	2.7	2.4	1.8
%Diff _{peak, 22}	3.4	2.3	2.3	2.3	2.4
%Diff _{peak, 28}	3.2	2.7	2.2	1.7	1.8
%Diff _{peak, 37}	4.4	4.3	3.0	2.9	2.3